Comparison of Newtonian and Non-Newtonian Oscillatory Flows Using the Lattice Boltzmann Method

J. Boyd[1], J.M. Buick[1] and S. Green[2]

[1] Physics and Electronics, [2]Human Biology, School of Biological, Biomedical and Molecular Sciences, University of New England, Armidale, Australia

Abstract— The lattice Boltzmann method incorporating a Casson non-Newtonian viscosity model for blood is used to compare two-dimensional Newtonian and non-Newtonian oscillatory flow simulations at Reynold's and Womersley's numbers corresponding to aorta and brachial artery blood flows. It is found that in both cases the Newtonian and non-Newtonian shear profiles exhibit differences, particularly near the vessel walls. This has implications for arterial simulations where shear stress is important.

Keywords— Lattice Boltzmann Method, Casson, oscillatory flow, non-Newtonian, arterial flow

I. INTRODUCTION

Atherosclerotic cardiovascular disease is a leading cause of morbidity in the industrialized world [1,2]. In the arterial circulation, local haemodynamics play an important role in the initiation and progression of vascular dysfunction and atherosclerosis [2]. To date, the description of local haemodynamics has been based on the assumption that blood behaves as a Newtonian fluid [3-6].

Blood is a concentrated suspension consisting of a number of formed elements suspended in plasma that exhibits non-Newtonian shear thinning behavior. Modelling blood as a Newtonian fluid is generally held to be a good first approximation, particularly when considering the velocity in the larger vessels [3]. However, wall shear in the artery has also been determined to be an important factor in the development of atherosclerosis [4-6]. This paper will examine whether the assumption of Newtonian viscosity is still valid for near wall shear stress in a two-dimensional oscillatory flow using the lattice Boltzmann method (LBM)

The LBM uses a modified molecular dynamics approach to simulate fluid flow and has been applied to many problems, including blood flow [7-11]. The simple lattice structure of the model, coupled with a sub-grid accurate extrapolation boundary scheme [12] makes the LBM suitable for modelling fluid flow in complicated geometries such as those found in arterial flow problems.

The LBM also has the advantage of being able to calculate the fluid shear stress at each node of the lattice [13], negating the need for time-consuming derivations of the shear from velocity field data. In addition the LBM can be easily adapted to implement shear dependent non-Newtonian flows.

II. THEORETICAL BACKGROUND

A. The Lattice Boltzmann Method

The lattice Boltzmann method [14] has been developed as an alternative method for simulating fluid flows. In the LBM particle distribution functions, $f_i(\mathbf{x}, t)$ at point $\mathbf{x}$ at time t evolve on a regular lattice. The subscript i denotes the lattice link the distribution function is on. The distributions interact on the lattice in a way that conserves mass, momentum, isotropy and Galilean invariance.

The evolution of the distribution functions on the lattice is governed by the discrete Boltzmann equation [14]

$$f_i(\mathbf{x} + \mathbf{e}_i, t+1) = f_i(\mathbf{x}, t) - \left(f_i^{eq}(\mathbf{x}, t) - f_i(\mathbf{x}, t) \right) \Big/ \tau, \ (1)$$

where τ is the relaxation time and f_i^{eq} will be discussed below. In this paper we use the D2Q9 lattice, a two-dimensional lattice with nine link directions $i = 0, \ldots, 8$ defined as:

$$\mathbf{e}_i = (0,0), \qquad\qquad (i = 0),$$

$$\mathbf{e}_i = (\cos(\pi(i-1)/2), \sin(\pi(i-1)/2)), \qquad (i = 1,2,3,4),$$

$$\mathbf{e}_i = \sqrt{2}(\cos[\pi(i-1)/2 + \pi/4], \sin[\pi(i-1)/2 + \pi/4]),$$

$$(i = 5,6,7,8), \quad (2)$$

The fluid density ρ and velocity $\mathbf{u}$ can be calculated directly from each node by $\rho = \sum_i f_i$ and $\rho\mathbf{u} = \sum_i f_i \mathbf{e}_i$. The distribution functions f_i can be expanded as $f_i = f_i^{eq} + f_i^{neq}$. The non-equilibrium part f_i^{neq} can be further expanded as $f_i^{neq} = \varepsilon f_i^{(1)} + \varepsilon^2 f_i^{(2)} + o(\varepsilon^3)$ where $\sum_i f_i^{(k)} = \sum_i f_i^{(k)} \mathbf{e}_i = 0$ for $k = 1,2$ and ε is the Knudson number.

The equilibrium form of the distribution function in two dimensions for the D2Q9 lattice is given by [15]

$$f_i^{eq}(x,t) = w_i \rho \left(1 + 3\mathbf{e}_i \cdot u + 9(\mathbf{e}_i \cdot u)^2 / 2 - 3u^2 / 2\right) \quad (3)$$

where $w_0 = 4/9$, $w_i = 1/9$ for $i = 1,2,3,4$ and $w_i = 1/36$ for $i = 5,6,7,8$. τ is related to the kinematic viscosity ν by

$$\nu = (2\tau - 1)/6 \quad (4)$$

The stress tensor for an incompressible fluid with pressure p is given by

$$\sigma_{\alpha\beta} = -p\delta_{\alpha\beta} + 2\nu S_{\alpha\beta} \quad (5)$$

where $\delta_{\alpha\beta}$ is the Kronecker delta and $S_{\alpha\beta} = \left(\nabla_\beta u_\alpha + \nabla_\alpha u_\beta\right)/2$ is the strain rate tensor. It can be shown [7] that $S_{\alpha\beta}$ can be calculated in the LBM by

$$S_{\alpha\beta} = -3\sum_i f_i^{(1)} \mathbf{e}_{i\alpha}\mathbf{e}_{i\beta} / 2\tau . \quad (6)$$

B. Casson Non-Newtonian Blood Viscosity model

In this paper the Casson shear rate dependent non-Newtonian blood viscosity model will be used [3,16]. In the following discussion we will denote the second invariant of the strain rate tensor as

$$D_{II} = \sum_{\alpha,\beta=1}^{2} S_{\alpha\beta}S_{\alpha\beta} . \quad (7)$$

The strain rate is then defined as $\dot{\gamma} = \sqrt{D_{II}}$.

The Casson model is broadly used to describe the shear thinning behavior of blood. In this model the apparent viscosity, η, is given by

$$\eta(\dot{\gamma}) = \left(k_0(c) + k_1(c)\sqrt{\dot{\gamma}}\right)^2 / \dot{\gamma} \quad (8)$$

where $k_0(c)$ and $k_1(c)$ are functions of the hematocrit c given by $k_0(c) = \left(a\zeta/ab - 1\right)\left(k_1(c)/\sqrt{\eta_p} - 1\right)$ and $k_1(c) = \sqrt{\eta_p / (1-c)^{ab-1}}$. Here, η_p is the plasma viscosity and a, b, ζ are constant parameters determined from physiological measurements. In this paper parameters of $k_0(c) = 0.1937$ and $k_1(c) = 0.055$ were used [16].

III. METHOD

Oscillatory Newtonian and non-Newtonian flows driven by a sinusoidally varying pressure gradient [17,18] in a rigid 2D pipe model were implemented using the LBM. The Womersley ($\alpha = L\sqrt{\pi/2T\nu}$) and Reynold's ($\mathrm{Re}_\delta = U_0\sqrt{T/\nu\pi}$) numbers were taken to be $\alpha = 15$, $\mathrm{Re}_\delta = 300$ for the aorta model and $\alpha = 3$, $\mathrm{Re}_\delta = 300$ for the brachial artery model. Here T is the period of the flow U_0 is the peak velocity and L is the pipe diameter. These numbers were chosen as typical physiological values for the aorta and brachial arteries, calculated from parameters in Haugen et al. [18] and Stoner et al. [19] respectively. T was taken to be 0.75 s. For the Casson model $\eta = k_1^2$, this limiting viscosity was taken to be the viscosity of the corresponding Newtonian flow. From equation (8) we see that $\eta \to \infty$ as $\dot{\gamma} \to 0$, thus a cut off was implemented to prevent numerical instabilities at zero shear rates. The effect of this cut off on the apparent viscosity profile can be seen in Figure 1d), varying this cut off did not significantly affect the velocity or shear profiles.

IV. RESULTS

Figure 1 shows the velocity profiles in the aorta model across the width of the pipe normalised by the pipe diameter. The peak velocity, a), time $0.1T$ later, b), and the corresponding shear and apparent viscosity profiles for these times, c) and d) respectively are shown. It is observed that the velocity profiles agree closely, with the biggest differences (1.6%) occurring near the peak velocity in Figure 1a). Similar behaviour was observed throughout the whole of the oscillation period.

Differences in the shear occur over most of the profile. The largest differences (9%) occur near the edge of the pipe. In general the Casson non-Newtonian model predicts higher shears throughout the period of flow. The Casson non-Newtonian shear is lower at radial positions of approximately ± 0.75, corresponding to peaks in the viscosity profile and a slight shift in the radial position of the velocity peaks in Figures 1 a) and b).

The peaks in the viscosity profile coincide with stationary points of the velocity profile. The satellite peaks in the viscosity profiles seen in Figures 1 c) and d) occur near the edges of the pipe and correspond to the regions where the greatest differences are observed in the velocity and shear profiles.

Figure 2 shows the velocity profiles in the brachial artery model at the peak velocity, a), at time $0.1T$ later, b), and the corresponding shear and apparent viscosity profiles for these times, c) and d) respectively. It is observed that at the peak velocity, Figure 2a), the velocity profiles match closely, however the predicted velocity profiles diverged significantly (9%) at lower velocities. This effect can be seen in Figure 2b).

The shear profiles differ over the whole of the pipe width, see Figures 2 c) and d). Once again the largest difference (12%) occur near the wall of the pipe. These differences persisted throughout the period of flow. The Casson non-Newtonian shear profile predicts larger shears than the corresponding Newtonian flow, as was observed in the aorta model.
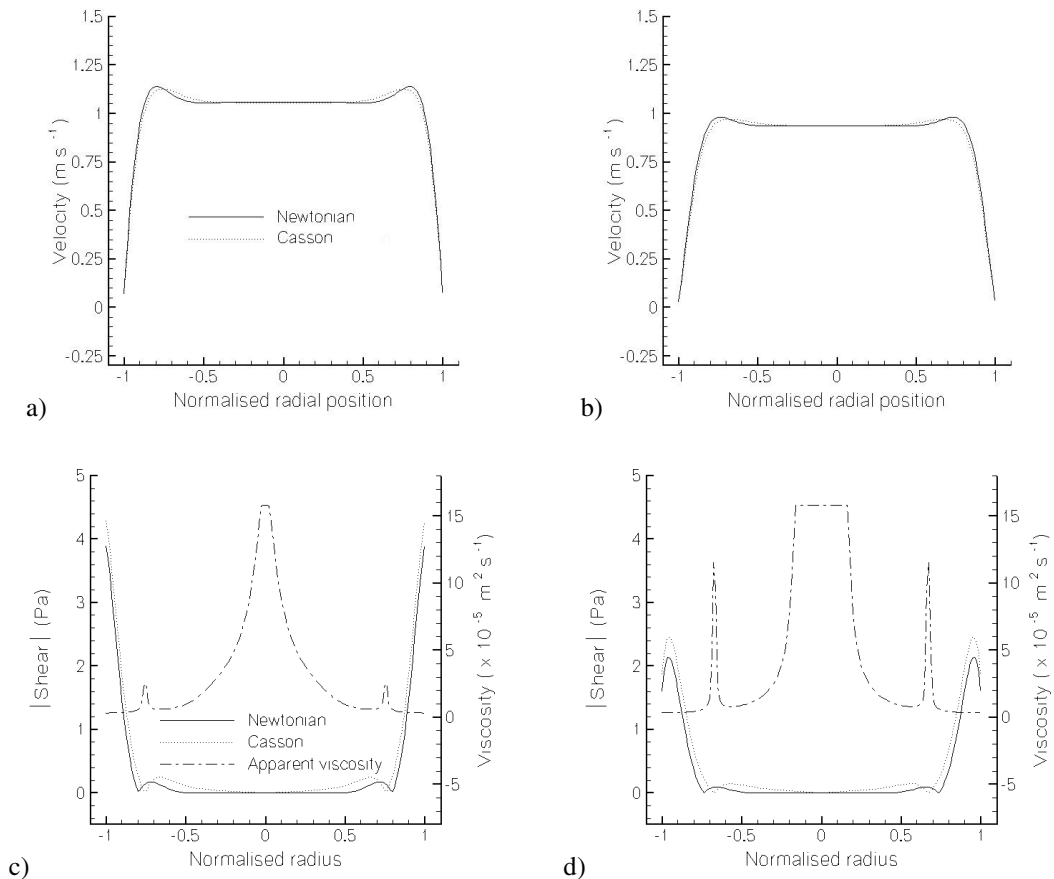
Fig 1: Aorta model velocity, shear and apparent viscosity profiles at peak velocity, a) and c), and at time $0.1T$ later, b) and d)

The viscosity profile also exhibited satellite peaks similar to those observed in the aorta model (data not shown). These peaks also corresponded to regions of lower Casson non-Newtonian shear and stationary points in the velocity profile.

III. Conclusions

Newtonian viscosity is generally assumed to be a good first approximation for large artery models. This approximation may be suitable for accurate velocity field predictions, however the results in this paper suggest that care should be taken with this assumption when shear dependant phenomena are being investigated.

Differences between Newtonian and Casson non-Newtonian velocities become more apparent in smaller arteries such as the brachial.

In general, the largest observed differences in shear profiles occurred near the walls of the vessel. Such differences may need to be taken into account when investigating hemodynamical influences on physiological processes such as atherosclerotic progression.

References

1. Murray C J L and Lopez A D. (1996) The global burden of disease: a comprehensive assessment of mortality and disability from diseases, injuries, and risk factors in 1990 and projected to 2020. Cambridge MA
2. Caro C G. (2001) Vascular fluid dynamics and vascular biology and disease. Math Method Appl Sci 24:1311-1324
3. Quarteroni A, Tuveri M and Veneziani A (2000) Computational vascular fluid dynamics: problems, models and methods. Comput Vis Sci 2:163-197
4. Malek A M, Alper S L and Izumo S (1999) Hemodynamic shear stress and its role in atherosclerosis. J Am Med Assoc 282:2035-2042
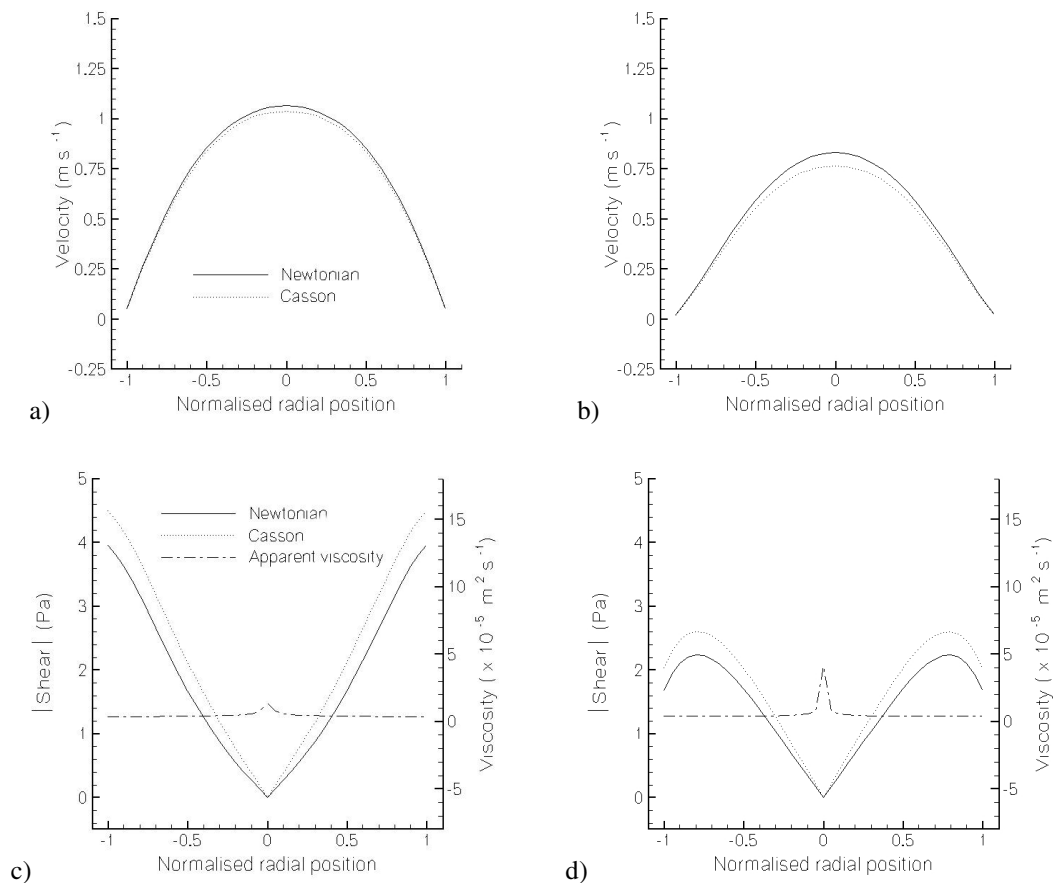
Fig 2: Brachial model velocity, shear and apparent viscosity profiles at peak velocity, a) and c), and at time $0.1T$ later, b) and d)

5. Asakura T and Karino T (1990) Flow patterns and spatial distribution of atherosclerotic lesions in human coronary arteries. Circ Res 66:1045-1066

6. Gnasso A et al (1997) In vivo association between low wall shear stress and plaque in subjects with asymmetrical carotid atherosclerosis. Stroke 28:993-998

7. Krafczyk M et al (2001) Two dimensional simulation of fluid-structure interaction using lattice-Boltzmann methods. Comput Struct 79:2031-2037

8. Boyd J, Buick J, Cosgrove J A and Stansell P (2005) Application of the lattice Boltzmann model to simulated stenosis growth in a two-dimensional carotid artery. Phys Med Biol 50:4783-4796

9. Lu X Y et al (2006) Lattice BGK simulations of the blood flow in elastic vessels. Chinese Phys Lett 23(3):738-741

10. Artoli A M et al (2004) Lattice BGK simulations of flow in a symmetric bifurcation. Future Gener Comp Sy 20(6):909-916

11. Li H B et al (2004) Lattice Boltzmann simulation on particle suspensions in a two-dimensional symmetric stenotic artery. Phys Rev E 69(3) Art. No. 031919 Part 1

12. Guo Z, Zheng C and Shi B (2002) An extrapolation method for boundary conditions in lattice Boltzmann method. Phys Fluids 14:2007-2010

13. Artoli A M (2003) Mesoscopic Computational Haemodynamics, Ponsen & Looijen, Wageningen

14. Chen S and Doolen G D (1998) Lattice Boltzmann method for fluid flows. Ann Rev Fluid Mech 30:329-364

15. Quian Y H, d'Humieres D and Lallemand P (1992) Lattice BGK models for Navier-Stokes equation. Europhys Lett 17:479-484

16. Perktold Km Resch M and Florian H (1991) Pulsatile non-Newtonian flow characteristics in a three-dimensional human carotid bifurcation model. J Biomech Eng 113:464-475

17. Cosgrove J A et al (2003) Application of the lattice Boltzmann method to transition in oscillatory channel flow. J Phys A 36:2609-2620

18. Buick J M and Greated C A (2000) Gravity in a lattice Boltzmann model. Phys Rev E 61:5307-5320

19. Haugen B O et al (2002) Blood Flow Velocity Profiles in the Aortic Annulus: a 2-Dimensional Freehand Color Flow Doppler Imaging Study. J Am Soc Echocardiog 15:328-333

20. Stoner L, Sabatier M, Edge K and McCully K (2004) Relationship between blood velocity and conduit artery diameter and the effects on vascular reponsiveness. J App Physiol 96:2139-2145

Address of the corresponding author:

Author: Mr. Joshua Boyd
Institute: Physics and Electronics, University of New England
Street:
City: Armidale, NSW, 2351
Country: Australia
Email: jboyd3@une.edu.au